Journal of Molecular Histology (2018) 49:277–287
https://doi.org/10.1007/s10735-018-9767-2

ORIGINAL PAPER

# Effects of CD100 promote wound healing in diabetic mice

**Fang Wang[1,2] · Bei Liu[1,3] · Zhou Yu[1] · Tong Wang[1] · Yajuan Song[1] · Ran Zhuang[4] · Yonghong Wu[3] · Yingjun Su[1] · Shuzhong Guo[1]**

Received: 22 December 2017 / Accepted: 12 March 2018 / Published online: 10 April 2018


## Abstract

Diabetes is a condition that causes delayed wound healing and results in chronic wounds. CD100 has been reported to promote and induce potent and obvious angiogenesis both in vivo and in vitro studies, the absence of which are a main cause of the diabetic chronic wound. In the present study, we investigated the effects of application of soluble CD100 on wound healing in diabetic mice. Four 5-mm full-thickness dermal wounds were made on each male db/db mouse. 12 mice from CD100 group were subcutaneously injected with 250 ng of CD100 (50 µl) per wound, in addition, 12 mice were injected with the same volume phosphate-balanced solution as the control. The animals were treated every other day until the wounds healed completely. Images were obtained to calculate the area ratio of the original area. HE and Masson's trichrome staining were used for histological examination. Collagen remodeling, angiogenesis and wound bed inflammation were evaluated by immunohistochemical staining and western blot. We demonstrated that CD100 had distinct functions during the wound healing process. Histological and western blotting analysis showed a more organized epithelium and dermis, more collagen fibers, higher angiogenesis and lower inflammation in the CD100 group than in the PBS group. These findings suggest that CD100 may accelerate wound healing in diabetic mice by promoting angiogenesis in the wound and by reducing the inflammatory response.

**Keywords** Wound healing · CD100 · Diabetes · Angiogenesis · Inflammation

## Abbreviations

| | |
|---|---|
| bFGF | Basic fibroblast growth factor |
| CD100 | Cluster of differentiation 100 |
| CD31 | Cluster of differentiation 31 |
| CD34 | Cluster of differentiation 34 |
| CD68 | Cluster of differentiation 68 |
| CD72 | Cluster of differentiation 72 |
| Col I | Collagen type I |
| Col III | Collagen type III |
| DAB | Diaminobenzidine |
| HGF | Human growth factor |
| IL-6 | Interleukin-6 |
| PBS | Phosphate-balanced solution |
| TNF-α | Tumor necrosis factor alpha |

Fang Wang and Bei Liu have contributed equally to this work.

**Electronic supplementary material** The online version of this article (https://doi.org/10.1007/s10735-018-9767-2) contains supplementary material, which is available to authorized users.

✉ Yingjun Su
xjzx2011@fmmu.edu.cn

✉ Shuzhong Guo
shuzhong@fmmu.edu.cn

Fang Wang
wangfang1956@163.com

Bei Liu
liubei83@163.com

[1] Department of Plastic and Reconstructive Surgery, Xijing Hospital, The Fourth Military Medical University, No. 127 Changle West Road, Xi'an 710032, Shaanxi, China

[2] Department of Medical Cosmetology, The First Affiliated Hospital of Xian Medical University, No. 48 Fenggao West Road, Xi'an 710000, Shaanxi, China

[3] Department of Medical Technology, Xian Medical University, No. 1 Xinwang Road, Xi'an 71000, Shaanxi, China

[4] Department of Transplantation Immunology Laboratory of Basic Medical College, The Fourth Military Medical University, No. 127 Changle Road, Xi'an 710032, Shaanxi, China

## Introduction

Diabetes mellitus (DM) is a metabolic disorder that occurs over a prolonged period of time. Multiple complications are associated with diabetes, and the chronic wound is one common, severe and serious long-term complication of advanced stage disease. The diabetic foot is the most common complication and the main cause of amputations associated with non-healing diabetic lower-extremity ulcers (Apelqvist 2012). The etiology of the diabetic chronic wound is complicated and involves various molecular and cellular mechanisms. In diabetic patients, vascular changes or damage lead to tissue ischemia, and the subsequent hypoxia contributes to delayed and non-healing wound closure (Algenstaedt et al. 2003). Cumulative studies have revealed that stimulation of angiogenesis during the wound repair process can efficiently accelerate wound healing in diabetic animals (An et al. 2015; Liu et al. 2014).

CD100, also known as Semaphorin 4D, is a member of the Semaphorin signaling protein family. As an axon guidance molecule in the central nervous system, CD100 is secreted by oligodendrocytes and can induce growth cone collapse by binding to the Plexin B1 receptor (Ito et al. 2006; Giacobini et al. 2008). In the immune system, CD100 activates B cells and dendritic cells by binding to CD72 (Ishida et al. 2003; Chabbert-de et al. 2005). However, one study has reported that CD100 plays an important role in the wound healing process by interacting with Plexin B2 during skin damage repair (Deborah et al. 2012). In addition, in vivo and in vitro studies have shown that CD100 can clearly promote angiogenesis or mimic events in angiogenesis (Basile et al. 2006; Fazzari et al. 2007).

Therefore, in the current study, we examined the effects of topical exogenous CD100 administration on wound healing in diabetic mice. Full-thickness dermal wounds were generated on db/db mice, and CD100 was subcutaneously injected. Various examinations were performed to evaluate the effects of CD100 on the wound healing process and to demonstrate the possible mechanism underlying the effects of topical application of exogenous CD100 in the diabetic mouse wound.

## Materials and methods

### Animals

Twenty-four 10-to-12-week-old leptin receptor-deficient male C57BL/6 mice (db/db; BKS.Cg-Dock7m+/+ Leprdb/JNju) and twenty 6-to-8-week-old db/m (heterozygote mice) mice were provided by the Model Animal Research Center of Nanjing University. All animals were housed separately at constant temperature and humidity under a 12-h light/dark cycle with ad libitum access to food and water. Mice were monitored for at least 2 weeks during the study. The mouse experimental protocols were approved and conducted in accordance with the Guide to the Care and Use of Experimental Animals of the Laboratory of Plastic Surgery in Xijing Hospital and the Committee of The Fourth Military Medical University.

### Wounding and treatment model

All the animals were weighed, measured for blood glucose with One Touch Ultra. Mice were anesthetized by inhalation of isoflurane to minimize animal suffering and distress. The fur from the scapular area to the lumbar area on the back of each mouse was shaved, and the stubble was eliminated with hair removal creams. The dorsal skin was washed with clean water and sterilized with 0.5% iodophor and 75% alcohol. Considering the limitation of the db/db mice number, four wounds were made with a 5-mm biopsy punch on the back of each mouse as previous studies (Ishrath et al. 2012; Conrotto et al. 2005). Full-thickness skin including epidermis, dermis and panniculus carnosus were removed (Galiano et al. 2004). Two wounds were generated in two locations that were 1 cm apart on each side of the back. The db/db mice were randomly allocated into two groups: the experimental group, which was treated with sCD100 (VaccinexInc, Rochester, New York, USA). The sCD100 used in the study was recombinant protein expressed in eukaryotic cells. (CD100 group, n = 12), and the control group, which was treated with phosphate-balanced solution (PBS) (PBS group, n = 12). Twenty db/m mice were performed the same operation. After the skin wounding, the db/db mice in the experimental group were subcutaneously injected with 50 µl of sCD100 (1.74 mg/ml, 40 µl sCD100 in 14 ml PBS) in each wound (250 ng/wound), and the db/db mice in the control group and db/m mice were subcutaneously injected with the same volume of PBS in each wound. The same treatment was performed every other day until the wound was completely healed.

### Assessment of wound healing

After wounding, the mice were anesthetized with isoflurane, and the wound surface areas were recorded. Photographs were taken immediately after wounding and every two days post-operation until the wound was completely healed by a digital camera while a ruler was placed near the wound. The wound areas were analyzed by Image-Pro Plus software. The original wound area was calculated immediately after wounding, and the wound closure area was expressed over

time as the percentage of the original wound area. The percentage of the wound closure area was calculated as

$$\{1 - [(\text{wound area})/(\text{original wound area})]\} \times 100\%.$$

### Wound tissue biopsy

On days 3, 7, 13, and 21, three mice were euthanized in each group. Then, the entire dorsal skin containing the wounds was separated and exposed under an operating microscope. Dissections were performed carefully to avoid breaking the blood vessels, and digital photographs were taken under the operating microscope. Sections of each wound and the surrounding tissue were obtained with an 8-mm biopsy punch.

### Morphological evaluation

Wound sections were fixed in 10% formalin and dehydrated in a graded ethanol series. The fixed tissues were embedded in paraffin per a standard procedure, and the paraffin tissue blocks were sectioned at a thickness of 4 μm. The slides were stained routinely with hematoxylin and eosin (HE) for examination by light microscopy. The HE results were examined and scored by two pathologists without knowledge of the previous treatment using a scoring system. The evaluated parameters contained reepithelialization and dermal granulation formation. The controls included the regions around the wound edges and the normal skin in each section. The HE analysis was performed with a semi-quantitative scoring approach (Altavilla et al. 2001; Niwano et al. 1996). First, a four-point scale was used to evaluate granulation tissue formation (1, thin granulation layer; 2, moderate granulation layer; 3, thick granulation layer; and 4, very thick granulation layer). Second, dermal and epidermal regeneration were assessed using a three-point scale (1, little regeneration; 2, moderate regeneration; and 3, complete regeneration). Slides were also stained with Masson's trichrome according to the manufacturer's protocol (Baso, Beijing, China) to demonstrate collagen deposition. Images were captured with a microscope.

### Immunohistochemistry (IHC) analysis

Samples were processed for IHC according to the instructions of the manufactures of the antibodies. Four-micron-thick sections on slides were deparaffinized and rehydrated. Then, antigen retrieval was performed by placing the slides in a 10 mmol/l sodium citrate buffer (pH 6.0) at 95 °C for 20 min, followed by 20 min of cooling. The slides were then washed in PBS, and non-specific binding sites were blocked with 1% BSA with 2% goat serum in PBS. The slides were incubated with the appropriate primary antibodies, namely, anti-CD34 (1:200, Boster Biological Technology Co. Ltd, Wuhan, China), anti-CD31 (1:200, Abcam Company, England), and anti-CD68 (1:200, Abcam Company, England), overnight at 4 °C. After washing, the slides were incubated with the biotinylated secondary antibody (Peroxidase/DAB+, Rabbit/Mouse) for 20 min at room temperature. The color was developed using a DAB substrate chromogen solution. The slides were counterstained with hematoxylin and observed with a light microscope. After obtained the fix representative images covering the majority of the wound bed at 400 magnification. The numbers of positive cells were counted in a blinded manner. The number of CD34-and CD31- positive cells in each field was used as an index of new vessel count (Rian et al. 2015) and vessels count respectively. CD68-positive cells were obtained from the number of positive cells in 5 hot spots in each slide (Hiroyuki et al. 2017). CD68 staining was performed to detect macrophages and evaluate changes in wound inflammation.

### Western blot analysis

The harvested wound tissues were homogenized in lysis buffer (50 mM Tris-HCl, 150 mM NaCl, and 0.05 M PMSF; pH 7.4). Lystaes were centrifuged at 10,000×*g* for 30 min at 4 °C. Equal amounts of proteins were electrophoresed 12% SDS-PAGE at 80 V for 40 min proteins were trans blotted on the PVDF membrane and processed with Col I, Col III, TNF-αand IL-6 (1:1000, Abcam Company, England) and GAPDH (1:5000, Bioworld Technology Inc, USA) antibodies and corresponding secondary antibodies (1:10,000). Signal intensity was quantified by image analyzer (Image J). The ratio of collagen I to collagen III was calculated using the following formula: ratio of collagen I to collagen III = expression levels of collagen I/collagen III × 100%.

### Statistical analysis

Statistical analyses were performed using GraphPad Prism 6 software. The data are expressed as the mean ± SD. Differences between groups were evaluated using a two-tailed unpaired Student's *t* test. A P-value of 0.05 or less was considered statistically significant.

## Results

### CD100 promotes wound healing in db/db mice

During the wound healing process, the wounds in the PBS and CD100 groups remained clean and dry, had few exudates, formed blood scabs and had no obvious contraction. As shown in Fig. 1a, wound area analysis indicated that there was no significant difference between the two db/db mice groups before 3 days, but a significant reduction was showed in CD100 group

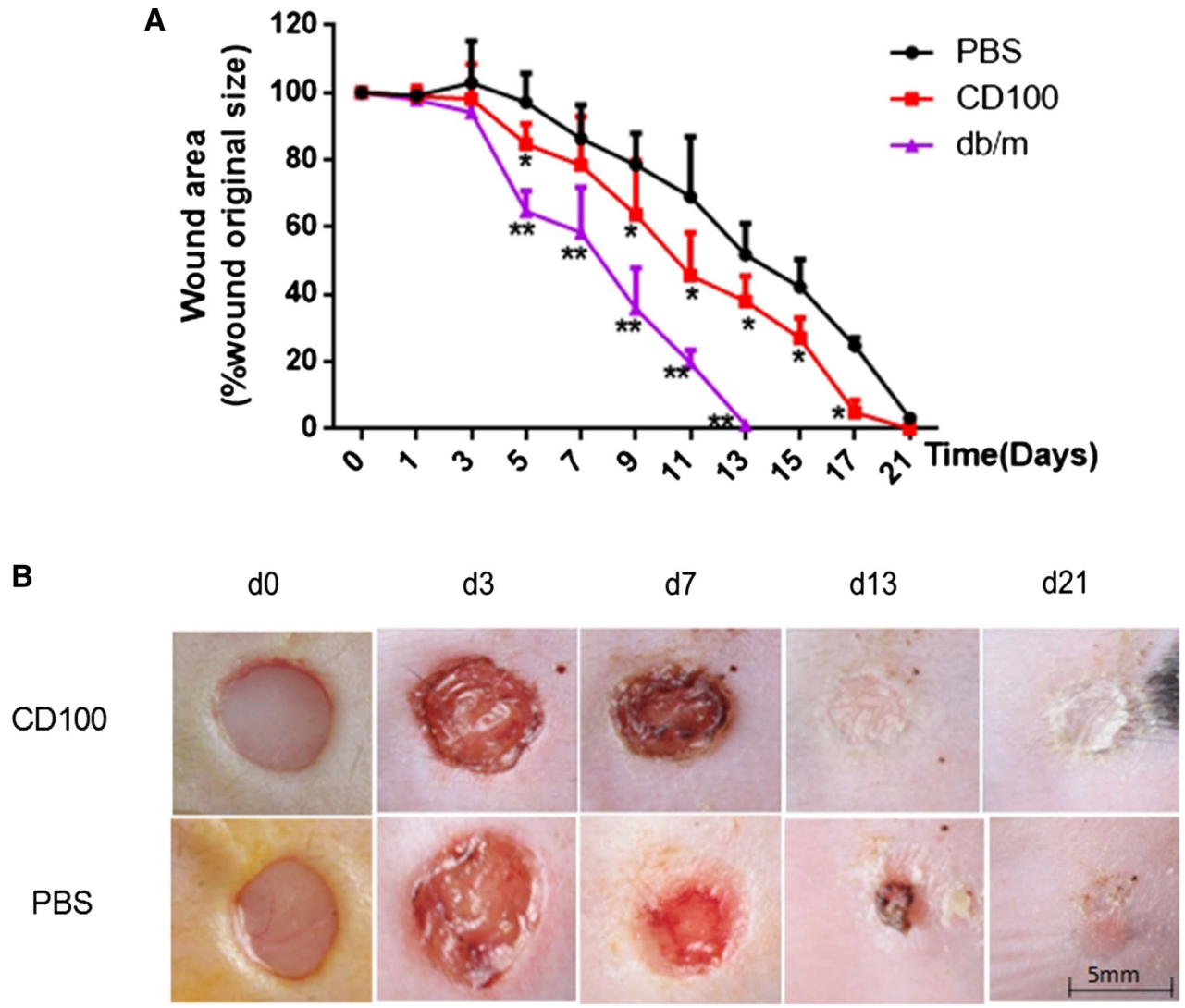


**Fig. 1** Effects of CD100 on wound closure of full-thickness excisional wounds in db/db mice. **a** Wound closure analysis. All wounds were measured on days 1, 3, 5, 7, 9, 11, 13, 15, 17 and 21 post-operation in db/db and db/m mice. The wound closure rate is plotted as the reduction percentage of the original wound area over time. The wound almost complete healing time for db/m mice is (13 ± 2) days, but the time was (21 ± 2) days (CD100-treat group) or longer (PBS-treat group) in db/db mice. The wound Values are presented as the mean ± SD (n = 12), and the level of significance is set at *$p < 0.05$ and **$p < 0.01$, the difference among these groups on day 3 is not statistically significant ($p > 0.05$). PBS—db/db mice treated with PBS, CD100—db/db mice treated with CD100, db/m—db/m mice treated with PBS. **b** Representative images of macroscopic view of db/db mice wound healing under the PBS and CD100 treatments on days 0 (before treatment), 3, 7, 13 and 21. Scale bar 5 mm

when compared with PBS group after day 9. The average wound area was significantly smaller in the db/m group than that in the two db/db groups beginning on day 5. Figure 1b showed the representative photograph of CD100 group and PBS treated db/db mice on day 3, 7, 13 and 21. (Data of db/m mice was not shown).

## CD100 dramatically enhances granulation tissue formation, dermis regeneration and collagen remodeling in db/db mice

As shown in Fig. 2a, the normal skin layers of db/db mice are thinner than that of db/m mice. As shown in Fig. 2b, both of the CD100 and PBS group had little epidermis and

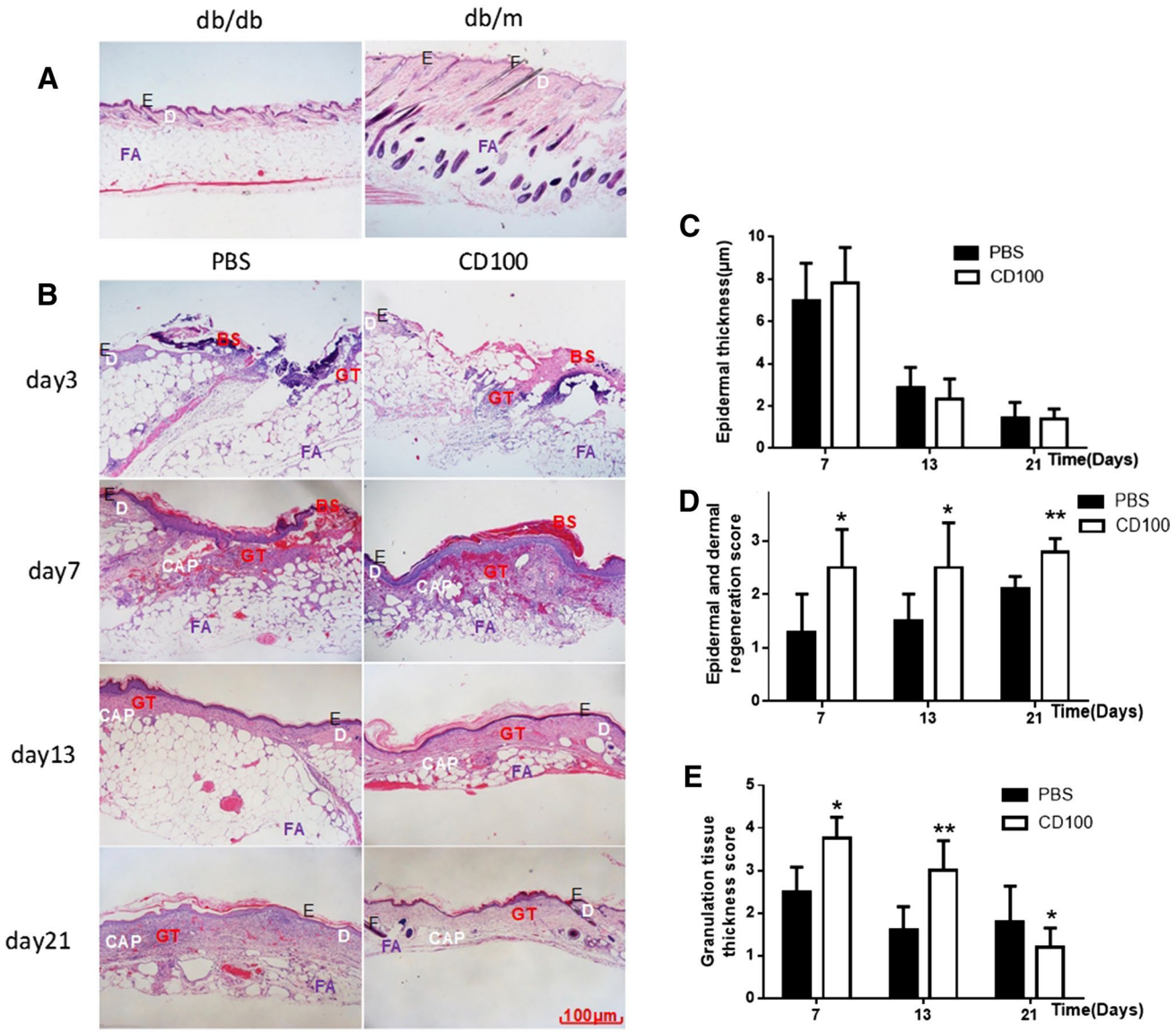


**Fig. 2** Effects of CD100 on histopathological examination of full-thickness excisional wounds in db/db mice. **a** HE-staining of the normal skin for db/m and db/db mice. **b** HE-staining of the db/db mice with CD100 or PBS treatment on days 3, 7, 13 and 21. Magnification ×40. Bars 100 μm. **c** Epidermal thickness of the wound of mice at days 7, 13 and 21. **d** Histological score of epidermis and dermis regeneration of the wound of mice at days 7, 13 and 21. **e** Histological score of granulation thickness of the wound of mice at days 7, 13 and 21. PBS—db/db mice treated with PBS, CD100—db/db mice treated with CD100. E—epidermis, D—dermis, F—hair follicle, FA—fat, GT—granulation tissue, BS—blood scab, CAP—capillaries. Values are presented as the mean ± SD (n = 12), and the level of significance is set at *$p < 0.05$ and **$p < 0.01$ compared to the PBS control group. The difference in epidermal thickness between the PBS and CD100 groups is statistically significant ($p > 0.05$)

dermis in the wound bed at day 3. However, on day 7, in the PBS group, the HE stains showed that the epidermal and dermal connections of the wounds were incomplete and that the granulation tissue showed medium thickness and a relatively loose structure beneath the epidermis and capillaries. Compared to the PBS group, in the CD100 group, the epidermis was closely connected to the dermis, and the formed granulation tissues were thicker, denser and more abundant in the capillaries. On day 13, the wound surfaces were completely covered by the epidermis in both the PBS and CD100 groups. Specifically, the dermal tissues of the CD100 group were thicker than those of the PBS group. On day 21, the dermal tissues were thick, and no follicle or other skin appendage was evident in the PBS group; however, both the epidermis and dermis were thinner in the CD100 group than in the PBS group, and new hair follicles were visible in the wound area in the CD100 group.

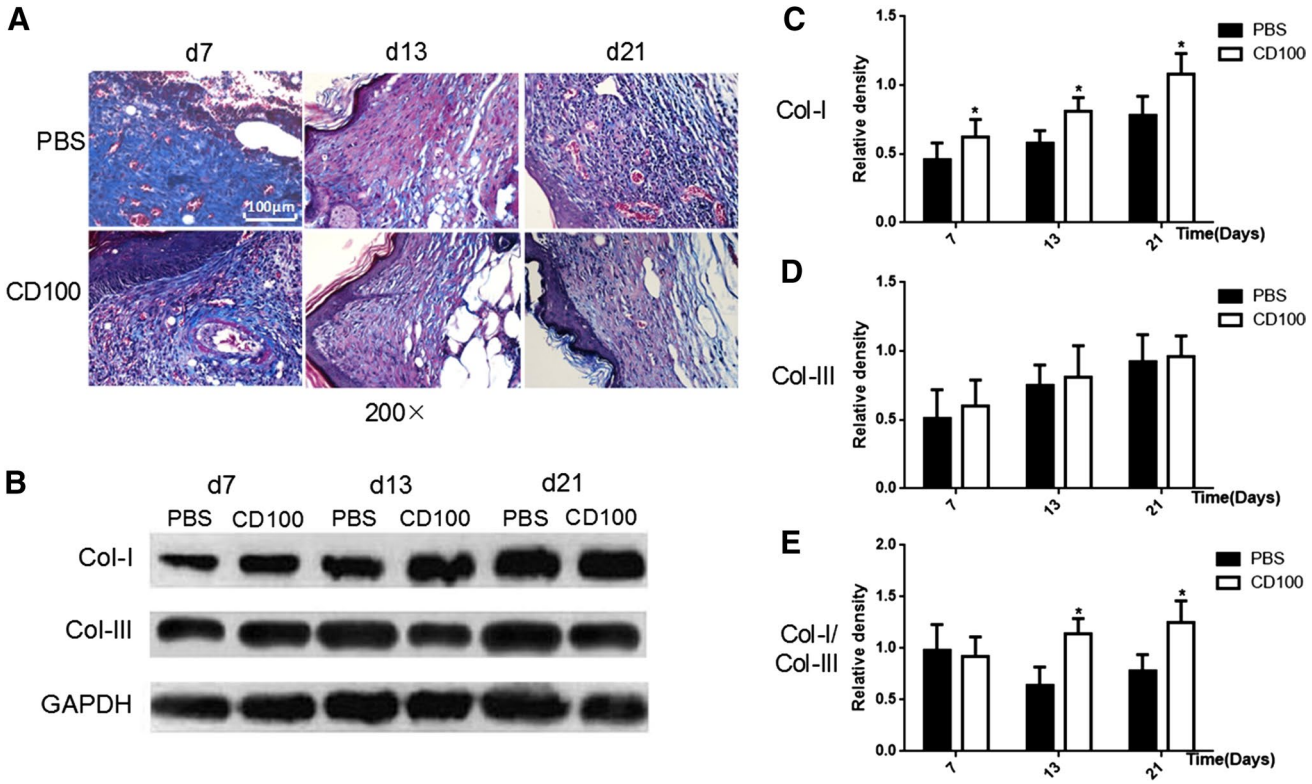


**Fig. 3** Masson's trichrome staining analysis and the expression of collagen I, III and ratio of collagen I/III in db/db mice. **a** Masson's trichrome-staining detection of the db/db mice with CD100 or PBS treatment on days 7, 13 and 21. Magnification ×200. Bars 100 μm. **b** Western blot gross images of collagen I and III in CD100 group and PBS group on the day 7, 13 and 21. **c** Expression of collagen I in different time of wound establishment. **d** Expression of collagen III in different time of wound establishment. **e** Ratio of collagen I to collagen III in CD100 group was higher than it in PBS-group during the diabetic wound healing. PBS—db/db mice treated with PBS, CD100—db/db mice treated with CD100. Values are presented as the mean ± SD (n = 12), and the level of significance is set at *$p < 0.05$ compared to the PBS control group. The difference of collagen III expression between the PBS and CD100 groups is statistically significant ($p > 0.05$)

As shown in Fig. 2c, the statistical results showed that the epidermis was thinner in the PBS group than that in the CD100 group on days 7, but it was thicker on day 13 and day 21. However, the difference was not statistically significant. Furthermore, as shown in Fig. 2d, the epidermis and dermis regeneration scores of the CD100 group were dramatically higher than those of the PBS group on days 7, 13 and 21. As shown in Fig. 2e, the granulation tissue thickness score of the CD100 group was greater than that of the PBS group on days 7 and 13 but less than that of the PBS group on day 21.

In addition, as shown in Fig. 3a, the Masson's trichrome staining results were similar to the HE staining results in the two groups at each time point. On day 7 after the operation, a few newly formed collagen tissue components were found in the wounds of the PBS and CD100 groups. On day 13, collagen synthesis, deposition and maturation were more orderly and pronounced in the CD100 group than in the PBS control group. On day 21, there were more collagen in these two groups, however, more newly and orderly and mature formed collagen tissues were found in the CD100 group than PBS group.

Collagen I is responsible for higher tensile strength, while collagen III is mainly found in early wound healing stages, and they keep a particular ratio in healthy skin. Moreover, as shown in Fig. 3b–e, western blotting demonstrated significant elevating expression of collagen type I and III in CD100 treated mice wound. Collagen I in CD100-group significantly increased compared to the PBS-group at day 7 ($0.62 \pm 0.13$ vs. $0.46 \pm 0.12$), day 13 ($0.81 \pm 0.10$ vs. $0.58 \pm 0.09$) and day 21 ($1.08 \pm 0.15$ vs. $0.78 \pm 0.14$) (Fig. 3c). In contrast, there is no statistically significant difference in collagen III expression between the two groups on day 7, 13, and 21 (Fig. 3d). In addition, the ratio of collagen I to collagen III in CD100-group was significantly higher than that in PBS-group at day 13 ($1.14 \pm 0.15$ vs. $0.64 \pm 0.18$), and day 21 ($1.25 \pm 0.21$ vs. $0.78 \pm 0.16$,), but the ratio difference was no significant statistical between two group on day 7 (Fig. 3e).

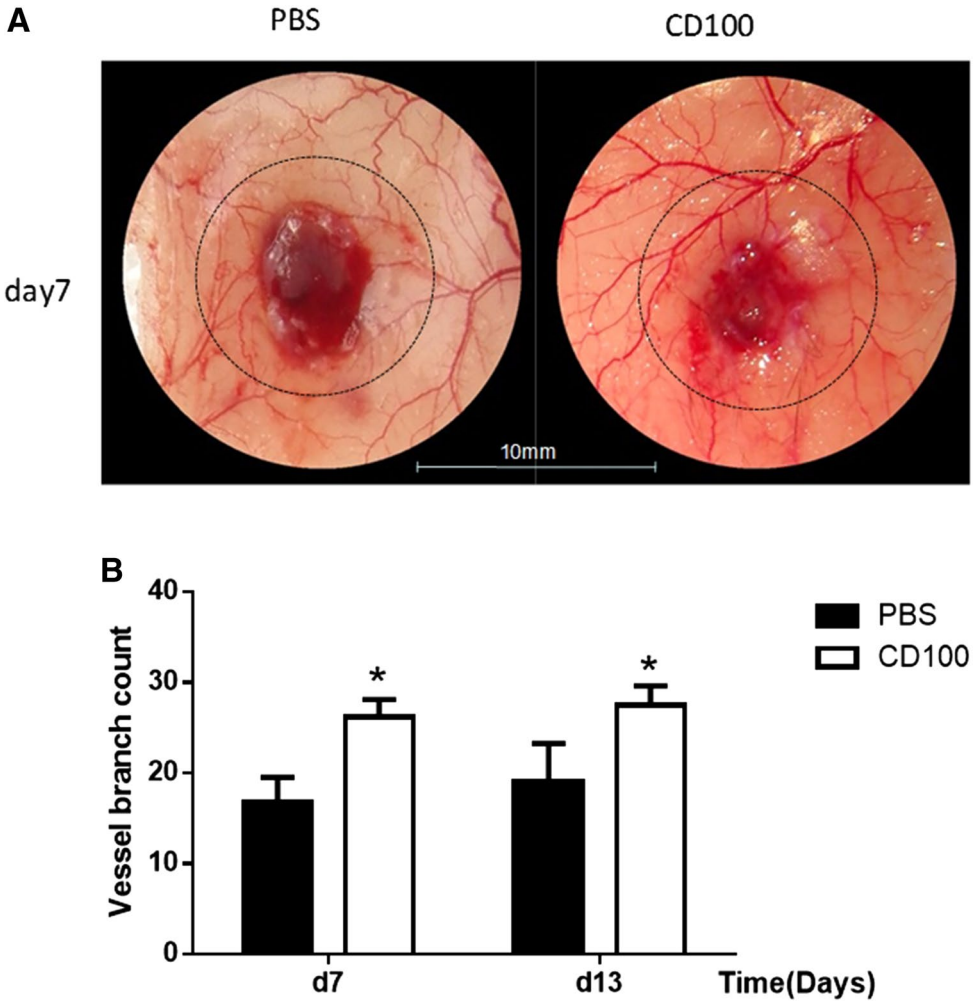


**Fig. 4** Effects of CD100 on angiogenesis in the macroscopic view of the full-thickness excisional wounds in the db/db mice. **a** Under the microscope, the blood vessels and blood circulation of the wounded tissues were evaluated for the PBS and CD100 treatment groups on days 7. Scale 10 μm. **b** Number of wound vessel branches on days 7 and 13. Values are presented as the mean ± SD (n = 12), and the level of significance is set at *p < 0.05 compared to the PBS control group. PBS—db/db mice treated with PBS, CD100—db/db mice treated with CD100

## CD100 enhances angiogenesis in db/db mice

The blood vessels and blood circulation of the wound next to dermis were observed under a microscope when the biopsy was performed. In addition, the examination showed that the CD100 group had a higher microvessel density and more abundant blood supply than the PBS group on days 7 (Fig. 4a). With the wound at the center, a 10-mm-diameter circle was drawn, and the number of vessel branches in the wound circle was determined. As shown in Fig. 4b, the results showed that the vascular branch number of the CD100 group was higher than that of the PBS group on day 7 and 13.

CD34 and CD31 IHC analysis was performed to evaluate wound angiogenesis (Fig. 5). Compared to the PBS treatment, the CD100 treatment showed increased blood vessel formation and a functional vascular architecture during the wound healing process. As shown in Fig. 5a, compared to the control PBS group, a high number of newly formed blood vessels and a high microvessel density were observed on days 7, 13 and 21 in the tissues from the CD100 treated wounds. As shown in Fig. 5b, both groups showed significant increases in the number of blood vessels on day 7. The number of blood vessels was obviously decreased on days 13 and 21 in each group relative to day 7. At the different time points, the number of new blood vessels was higher in the CD100 group than in the PBS group.

As shown in Fig. 5c, d, the result of CD31 staining was consistent with the CD34 staining. Compared to the PBS group, a higher number/field of newly formed blood vessels and a higher microvessel density were observed in CD100 group on days 7. The results of days 13 and 21 were similar to day 7, but the total number/field of the two groups were decreased compared to those on day 7 (Fig. 5c). As shown in Fig. 5d, both groups showed significant increases in the capillary number/field on day 7. The capillary number/field was obviously decreased on days 13 and 21 in each group compared to day 7. At each point, the capillary number/field was higher in CD100 group than those in PBS group.

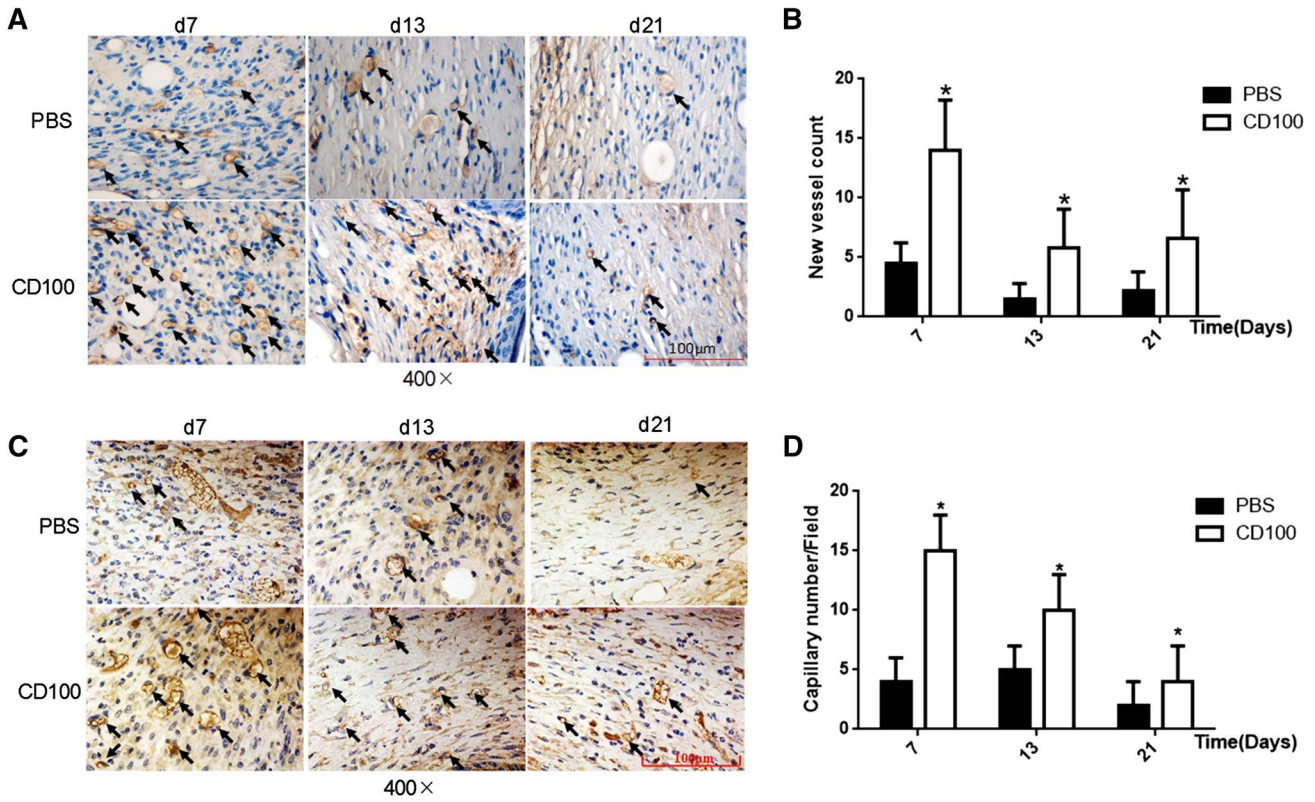


**Fig. 5** CD34 and CD31 staining analysis. **a** IHC results showing the CD34-stained wound tissues from days 7, 13 and 21. The black arrows indicate the blood vessels in the PBS- and CD100-treated wounds. Magnification ×400. Bars 100 μm. **b** Number of CD34-positive cells in the wound tissues on days 3, 7, 13 and 21. The CD100 treatment was associated with a higher number of CD34-positive cells than the PBS treatment. **c** IHC results showing the CD31-stained wound tissues on days 7, 13 and 21. The black arrows indicate the blood vessels/field in the PBS- and CD100-treated wounds. Magnification ×400. Bars 100 μm. **d** Capillary number/field in the wound tissues on days 7, 13 and 21. The CD100 treatment was associated with a higher capillary number/field than the PBS treatment. Values are presented as the mean ± SD (n = 12), and the level of significance is set at *$p < 0.05$ compared to the control. PBS—db/db mice treated with PBS, CD100— db/db mice treated with CD100

## CD100 decreases inflammation in wound healing in db/db mice

Macrophages and monocytes stained with CD68 were used to evaluate wound inflammation. A higher number of CD68-positive cells were observed in the tissues from the CD100-treated wounds than in those of the control on days 7, 13, 21 (Fig. 6a). In addition, as shown in Fig. 6b, our data clearly demonstrated that the CD68-positive cell number was maintained at a high level on days 7 and 13 in the PBS group. The CD68-positive cell number of the CD100 group was significantly lower than that of the PBS group on days 7 and 13. The CD68-positive cells were obviously decreased in both groups, and the number in the CD100 group was still lower than the number in the PBS group on day 21. The significant elevation in the number of CD68-positive cells on days 7 and 13 and the significant reduction in the number of CD68-positive cells on day 21 suggest that CD100 suppresses inflammation and promotes the wound repair process in db/db mice.

Moreover, as shown in Fig. 6c–e, western blotting demonstrated significant decreased expression of TNF-α and IL-6 in CD100 treated mice wound bed than those in PBS group. Compared to the PBS-group, expression of TNF-α in CD100 group were lower at day 7, day 13 and day 21 (Fig. 6c, d). The level of IL-6 expression also decreased in CD100 group on each time point than those of PBS group.

## Discussion

Wound healing is a complex, highly coordinated and ordered dynamic process that includes four phases: hemostasis or coagulation, inflammation, proliferation and remodeling (Gurtner et al. 2008; Barrientos et al. 2008; Zhao et al. 2017). Ischemia (reduced blood circulation and reduced angiogenesis), infection and neuropathy are the three main causes of diabetic delayed healing and the unhealed wound (Bruhn et al. 2012; Yang et al. 2017). Incurable diabetic wounds are mostly associated with

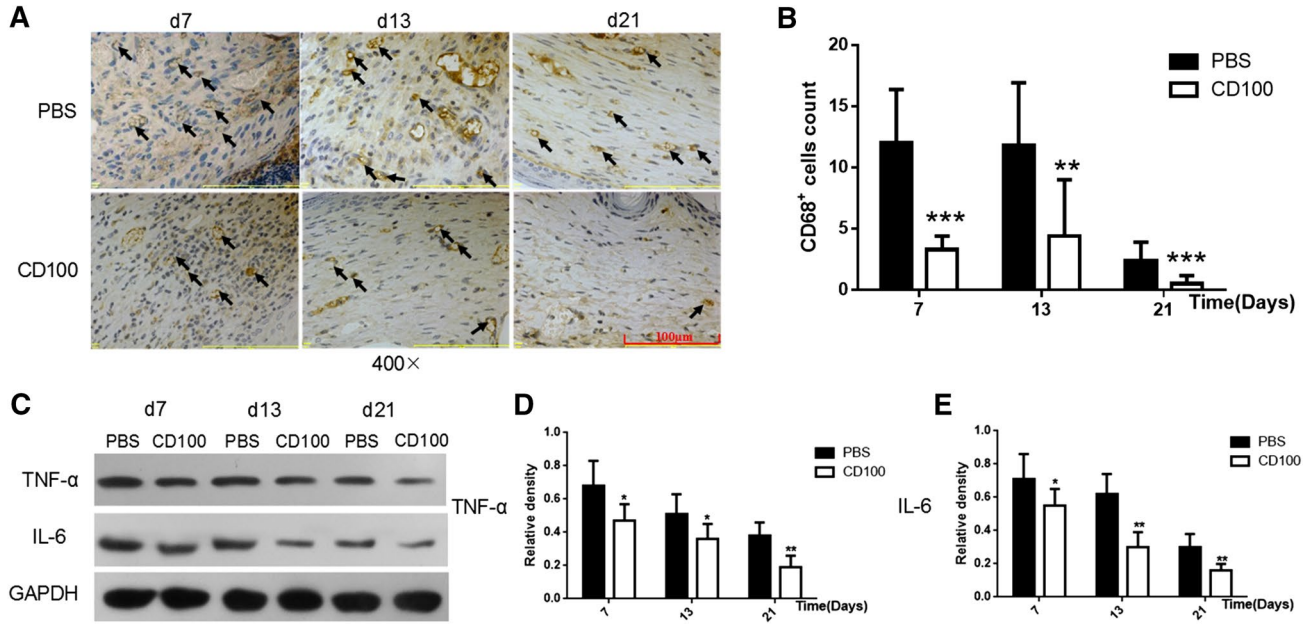


**Fig. 6** CD68 staining analysis and the expression of TNF-α and IL-6 in db/db mice. **a** CD68-stained tissues show the infiltration of macrophages/monocytes on days 7, 13 and 21. The black arrows indicate the accumulation of macrophages/monocytes in the PBS- and CD100-treated wounds. Magnification ×400. Bars 100 μm. **b** Number of CD68-positive cells present in the wound tissues on days 7, 13 and 21. The CD100 treatment showed a lower number of CD68-positive cells than the PBS treatment. **c** Western blot gross images of TNF-α and IL-6 in CD100 group and PBS group on the day 7, 13 and 21. **d** Expression of TNF-αin different time of wound establishment. **e** Expression of IL-6 in different time of wound establishment. PBS—db/db mice treated with PBS, CD100—db/db mice treated with CD100. Values are presented as the mean ± SD (n = 12), and the level of significance is set at *p < 0.05, **p < 0.01 and ***p < 0.001 compared to the control. PBS—db/db mice treated with PBS, CD100—db/db mice treated with CD100

regional ischemia, regional hypoxia and edema, and the wound healing process is prolonged during the period of inflammation (Martin et al. 2003; Snyder 2005). Therefore, multiple studies have attempted to increase angiogenesis and reduce inflammation to promote diabetic wound healing. However, in the clinic, various problems have become apparent with the use of growth factors or cytokines during treatment of chronic wounds. One serious problem involves efficacy, where the clinical curative effect of exogenous growth factors is not as high as the experimental effect (Diegelmann and Evans 2004; Shu et al. 2016). Hence, diabetic wound healing presents a significant unmet medical need.

CD100 is a class 4 Semaphorin family member and a type I membrane molecule. CD100 is widely expressed on immune cells and platelets (Zhu et al. 2007, 2009). A proteolytic site exists in the extracellular domain of CD100, and hydrolysis of CD100 with a proteolytic enzyme results in a soluble CD100 product. Therefore, two forms of CD100 exist: the membrane form (mCD100) and the soluble form (sCD100). sCD100 also has biological activity. In this study, we applied sCD100 that had been recombinantly expressed in eukaryotic cells to the diabetic wounds of mice. Compared with the control group, our data show that sCD100 has little obvious impact on re-epithelization and dramatically enhances granulation tissue formation, epidermis and dermis regeneration and collagen remodeling in diabetic mice.

In addition, our study has shown that CD100 significantly promotes angiogenesis in diabetic wounds. After skin injury, granulation tissue is formed in the process of wound healing, and new blood vessels are an important component of granulation tissue (Zhao et al. 2016). Angiogenesis is a crucial event in wound healing and forms new blood vessels from pre-existing vessels. In the wound healing process, angiogenesis is influenced and regulated by a large number of cells and cytokines (Li et al. 2008). Endothelial cells express Plexin B1, which is a high-affinity receptor of CD100 (Kumanogoh and Kikutani 2004). After CD100 binds to Plexin B1, the CD100-Plexin B1 complex not only enhances the cytoskeletal reorganization and migration of the vascular endothelial cell (Lai et al. 2009; Basile et al. 2005; Binmadi et al. 2011) but also promotes the formation of the capillary lumen and branch structure (Basile et al. 2004). Conrotto et al. reported that sCD100 had a strong effect on angiogenesis after embedding sCD100-containing Matrigel subcutaneously into the backs of mice (Conrotto et al. 2005). Meanwhile, data from chick embryo chorioallantoic membrane experiments have also confirmed this observation. Notably, the angiogenesis promoting effects of sCD100 depend on several

known angiogenesis promoting factors such as bFGF and HGF, but sCD100 does not upregulate the expression levels of these factors (Doupis et al. 2011). One study revealed that treatment with sCD100 alone clearly promoted angiogenesis (Falanga 2005). Our data are consistent with the data of former studies. CD100 significantly accelerates wound healing in diabetic mice, which may be due to the promotion of angiogenesis.

Our study also found that CD100 significantly reduced the inflammatory response in the diabetic wound. Studies have shown that diabetic wounds have more inflammatory cells in their epithelial tissues than non-diabetic wounds during the same period (Ahmed and ShahSaeid 2017). Moreover, the serum levels of pro-inflammatory factors such as IL-6 and TNF alpha are also significantly higher in diabetic wounds than in non-diabetic wounds (Tsubame et al. 2017).

An excessive and sustained inflammatory response is not conducive to wound healing as the response delays healing. mCD100 is highly expressed on the surfaces of activated T and B cells, and a low-affinity receptor of CD100, CD72, is expressed on dendritic cells and mononuclear macrophages (Smith et al. 2011). During the immune response, CD100 regulates the immune response by promoting the maturation of antigen presenting cells (mononuclear macrophages and dendritic cells) and the release of pro-inflammatory cytokines (Giraudon et al. 2004). The number of dendritic cells in CD100–/– mice is remarkably reduced in response to allogenic antigen stimulation, and the expression of co-stimulus molecules and IL-12 is also impaired (Kumanogoh et al. 2002). In our study, the application of exogenous sCD100 greatly reduced the inflammatory response in diabetic mice. Mechanistically, we hypothesize that the signal transmission of CD100 depends on the interaction between the mCD100 molecules on T cells and B cells and the CD72 molecules on antigen presenting cells. Contacts among T cells, B cells and antigen presenting cells are especially needed during this period. During application of exogenous sCD100, the connections between the mCD100 molecules and the CD72 antigen presenting cell surface receptors are competitively blocked. As a result, the excessive inflammatory reaction is inhibited, and wound healing is promoted toward the stages of proliferation and remodeling.

In summary, application of exogenous sCD100 enhances angiogenesis, reduces the inflammatory response and significantly promotes the healing process of the diabetic wound in mice. Therefore, sCD100 may be a new therapeutic target for clinical treatment of the chronic diabetic wound.

**Acknowledgements** This work was supported by the National Natural Science Foundation of China (81401598). The authors would like to thank Prof. Yi Chenggang for helpful discussions of the data and Dr. Chenlin and Liang Yingzi for assistance with the morphological evaluation.

## Compliance with ethical standards

**Conflict of interest** The authors declare that they have no conflicts of interest to disclose.

## References

Ahmed S, ShahSaeid AN (2017) The role of phytochemicals in the inflammatory phase of wound healing. Int J Mol Sci 18(5):1068

Algenstaedt P, Schaefer C, Biermann T, Hamann A, Schwarzloh B, Greten H, Ruther W et al (2003) Microvascular alterations in diabetic mice correlate with level of hyperglycemia. Diabetes 52(2):542–549

Altavilla D, Saitta A, Cucinotta D, Galeano M, Deodato B, Colonna M, Squadrito F et al (2001) Inhibition of lipid peroxidation restores impaired vascular endothelial growth factor expression and stimulates wound healing and angiogenesis in the genetically diabetic mouse. Diabetes 50(3):667–674

An YL, Wei W, Jing H, Ming LG, Liu SY, Jin Y (2015) Bone marrow mesenchymal stem cell aggregate: an optimal cell therapy for full-layer cutaneous wound vascularization and regeneration. Sci Rep 5:17036

Apelqvist J (2012) Diagnostics and treatment of the diabetic foot. Endocrine 41(3):384–397

Barrientos S, Stojadinovic O, Golinko MS, Brem H, Tomic-Canic M (2008) Growth factors and cytokines in wound healing. Wound Repair Regen 16(5):585–601

Basile JR, Barac A, Zhu TQ, Guan KL, Gutkind JS (2004) Class IV semaphorins promote angiogenesis by stimulating Rho-initiated pathways through plexin-B. Cancer Res 64(15):5212–5224

Basile JR, Afkhami T, Gutkind JS (2005) Semaphorin 4D/plexin-B1 induces endothelial cell migration through the activation of PYK2, Src, and the phosphatidylinositol 3-kinase-Akt pathway. Mol Cell Biol 25(16):6889–6898

Basile JR, Castilho RM, Williams VP, Gutkind JS (2006) Semaphorin 4D provides a link between axon guidance processes and tumor-induced angiogenesis. Proc Natl Acad Sci USA 103(24):9017–9022

Binmadi NO, Proia P, Zhou H, Yang YH, Basile JR (2011) Rho-mediated activation of PI(4)P5K and lipid second messengers is necessary for promotion of angiogenesis by Semaphorin 4D. Angiogenesis 14(3):309–319

Bruhn OB, Korzon BA, Gabig CM, Olszewski P, Węgrzyn A, Jakóbkiewicz BJ (2012) Molecular factors involved in the development of diabetic foot syndrome. Acta Biochim Pol 59(4):507–513

Chabbert-de PI, Marie-Cardine A, Pasterkamp RJ, Schiavon V, Tamagnone L, Thomasset N, Boumsell L et al (2005) Soluble CD100 functions on human monocytes and immature dendritic cells require plexin C1 and plexin B1, respectively. Int Immunol 17:439–447

Conrotto P, Valdembri D, Corso S, Sweini G, Tamagone L, Comoglio PM, Giordano S et al (2005) Sema4D induces angiogenesis through Met recruitment by Plexin B1. Blood 105(11):4321–4329

Deborah AW, Megumi W, Olivia G, Stephanie E, Rieder GS, Shane JF, Wendy LH et al (2012) The CD100 receptor interacts with its plexin B2 ligand to regulate epidermal γδ T cell function. Immunity 37(2):314–325

Diegelmann RF, Evans MC (2004) Wound healing: an overview of acute, fibrotic and delayed healing. Front Biosci 9:283–289

Doupis J, Rahangdale S, Gnardellis C, Pena SE, Malhotra A, Veves A (2011) Effects of diabetes and obesity on vascular reactivity, inflammatory cytokines, and growth factors. Obesity (Silver Spring) 19(4):729–735

Falanga V (2005) Wound healing and its impairment in the diabetic foot. Lancet 366(9498):1736–1743

Fazzari P, Penachioni J, Gianola S, Rossi F, Eickholt B, Maina F, Tamagnone L et al (2007) Plexin-B1 plays a redundant role during mouse development and in tumour angiogenesis. BMC Dev Biol 7:55

Galiano RD, Michaels J, Dobryansky M, Levine JP, Gurtner GC (2004) Quantitative and reproducible murine model of excisional wound healing. Wound Repair Regen 12:485–492

Giacobini P, Messina A, Morello F, Ferraris N, Corso S, Penachioni J et al (2008) Semaphorin 4D regulates gonadotropin hormone-releasing hormone-1 neuronal migration through PlexinB1-Met complex. J Cell Biol 183:555–566

Giraudon P, Vincent P, Vuaillat C (2004) Semaphorin CD100 from activated T lymphocytes induces process extension collapse in oligodendrocytes and death of immature neural cells. J Immunol 172(2):1246–1255

Gurtner GC, Werner S, Barrandon Y, Longaker MT (2008) Wound repair and regeneration. Nature 453(7193):314–321

Hiroyuki K, Yukiomi N, Taeko Y et al (2017) Influence of nicotine on choline-deficient, L-amino acid-defined diet-induced non-alcoholic steatohepatitis in rats. PLoS ONE 12(6):e0180475

Ishida I, Kumanogoh A, Suzuki K, Akahani S, Noda K, Kikutani H (2003) Involvement of CD100, a lymphocyte semaphorin, in the activation of the human immune system via CD72: implications for the regulation of immune and inflammatory responses. Int Immunol 15:1027–1034

Ishrath A, Vivekananda GS, Jacob G, Verena P, Claus PS, Sergiu-Bogdan C, Kerstin B, Elisabete AF (2012) Carnosine enhances diabetic wound healing in the db/db mouse model of type 2 diabetes. Amino Acids 43:127–134

Ito Y, Oinuma I, Katoh H, Kaibuchi K, Negishi M (2006) Sema4D/plexin-B1 activates GSK-3β through R-Ras GAP activity inducing growth cone collapse. EMBO Rep 7(7):704–709

Kumanogoh A, Kikutani H (2004) Biological functions and signaling of a transmembrane semaphorin, CD100/Sema4D. Cell Mol Life Sci 61(3):292–300

Kumanogoh A, Suzuki K, Ch'ng ES, Watanabe C, Marukawa S, Takegahara N, Kikutani H et al (2002) Requirement for the lymphocyte semaphorin, CD100, in the induction of antigen-specific T cells and the maturation of dendritic cells. J Immunol 169(3):1175–1181

Lai AZ, Abella JV, Park M (2009) Crosstalk in Met receptor oncogenesis. Trends Cell Biol 19(10):542–551

Li XY, Chen SZ, Li WZ, Li YJ, Lv XX, Li J, Li JQ et al (2008) Differentiation of the pericyte in wound healing: The precursor, the process, and the role of the vascular endothelial cell view issue TOC. Wound Repair Regen 16(3):346–355

Liu H, Duan ZL, Tang J, Lv QM, Rong MQ, Lai R (2014) A short peptide from frog skin accelerates diabetic wound healing. FEBS J 281(20):4633–4643

Martin A, Komada MR, Sane DC (2003) Abnormal angiogenesis in diabetes mellitus. Med Res Rev 23(2):117–145

Niwano Y, Koga H, Sakai A, Kanai K, Hamaguchi H, Uchida M, Tachikawa T (1996) Wound healing effect of malotilate in rats. Arzneimittel-forschung 46(4):450–455

Rian QL, Ryan MS, James M et al (2015) Hagberg. Chronic endurance exercise affects paracrine action of CD31+ and CD34+ cells on endothelial tube formation. Am J Physiol Heart Circ Physiol 309(3):H409-H420

Shu C, Smith SM, Melrose J (2016) The heparan sulphate deficient Hspg2 exon 3 null mouse displays reduced deposition of TGF-β1 in skin compared to C57BL/6 wild type mice. J Mol Histol 47(3):365–374

Smith EP, Shanks K, Lipsky MM, DeTolla LJ, Keegan AD, Chapoval SP (2011) Expression of neuroimmune semaphorins 4A and 4D and their receptors in the lung is enhanced by allergen and vascular endothelial growth factor. BMC Immunol 12:30

Snyder RJ (2005) Treatment of nonhealing ulcers with allografts. Clin Dermatol 23(4):388–395

Tsubame NYS, Kanazawa S, Makiko K, Kayoko O, Lin L, Ayato H, Rica T et al (2017) Interleukin-6 stimulates Akt and p38 MAPK phosphorylation and fibroblast migration in non-diabetic but not diabetic mice. PLoS ONE 12(5):e0178232

Yang L, Zheng Z, Zhou Q, Bai X, Fan L, Yang C, Su L, Hu D (2017) miR-155 promotes cutaneous wound healing through enhanced keratinocytes migration by MMP-2. J Mol Histol 48(2):147–155

Zhao RL, Liang H, Clarke E, Jackson C, Xue ML (2016) Inflammation in chronic wounds. Int J Mol Sci 17(2085):1–14

Zhao B, Zhang Y, Han S, Zhang W, Zhou Q, Guan H, Liu J, Shi J, Su L, Hu D (2017) Exosomes derived from human amniotic epithelial cells accelerate wound healing and inhibit scar formation. J Mol Histol 48(2):121–132

Zhu L, Bergmeier W, Wu J, Jiang H, Stalker TJ, Cieslak M, Kikutani H et al (2007) Regulated surface expression and shedding support a dual role for semaphorin 4D in platelet responses to vascular injury. Proc Natl Acad Sci 104(5):1621–1626

Zhu L, Stalker TJ, Fong KP, Jiang H, Tran A, Crichton I, Kikutani H et al (2009) Disruption of SEMA4D ameliorates interaction that accelerates atherosclerosis. Cardiovasc Res 105(3):361–371